Available online at www.sciencedirect.com
SCIENCE DIRECT®
Journal of Sound and Vibration 280 (2005) 945–964
JOURNAL OF SOUND AND VIBRATION
www.elsevier.com/locate/jsvi

Dynamic stability of rotating blades (beams) eccentrically clamped to a shaft with fluctuating speed

Ö. Turhan*, G. Bulut

Faculty of Mechanical Engineering, Istanbul Technical University, Gümüşsuyu 34439, Istanbul, Turkey

Received 8 August 2003; accepted 22 December 2003
Available online 12 October 2004

Abstract

In-plane bending vibrations of a beam rotating with a periodically fluctuating speed are considered. The partial differential equation of motion is discretisized via Galerkin's method and a set of Mathieu–Hill equations is obtained. The constant speed rotation problem is reviewed and its reflections onto the fluctuating speed problem are underlined. Dynamic stability analysis is performed via a monodromy matrix method and a generalized Bolotin method. Examples of stability charts are worked out reflecting stability's dependence on various pairs of system parameters.

1. Introduction

Since the pioneering work of Southwell and Gaugh [1] the vibration problem of rotating beams has been a subject of extensive research due to a number of very important applications such as helicopter and turbine blades, appendages of spinning satellites and also perhaps to its challenging mathematical aspect appealing to mathematical physicists.

Along with the fundamental problem of determining the natural frequencies of the in and out-of-rotation plane bending vibrations of centrically or eccentrically clamped beams [1–14], two subsidiary problems have been addressed in the literature. These are the buckling problem of eccentrically clamped, inward-oriented beams, [6,9,11,12,15,16–21], and the ''tuning'' problem

*Corresponding author.
E-mail address: turhanoz@itu.edu.tr (Ö. Turhan).

0022-460X/$ - see front matter © 2004 Elsevier Ltd. All rights reserved.
doi:10.1016/j.jsv.2003.12.053

[6,14]. Various analysis methods have been used in these studies, among which are the method of successive approximations [15], Rayleigh–Ritz method [8], Galerkin's method [6,14,16], perturbation methods [4,9,11,17,18,20], integrating matrix methods [19,21], Frobenius series [7,10,12] and finite element method [5,13].

A common feature of the above-referenced studies is that they all assume the beam to rotate at a constant rate. Al-Nassar and Al-Bedoor [22] have, on the other hand, recently attracted attention to the effect of the driving shaft's torsional vibrations on the bending vibrations of rotating blades. They have shown through numerical simulations of a single-degree-of-freedom simplified model that the vibrations of the shaft may be a source of instability for the blades.

Inspired by the above work, the present study considers the effect of a speed fluctuation in the driving shaft on the in-plane bending vibrations of rotating blades. The blades are assumed to be possibly eccentrically clamped uniform Euler–Bernouilli beams made of a Kelvin–Voigt material and a discrete mathematical model for their bending vibrations is obtained through Galerkin's method. It is shown that the dynamical behaviour of the system is governed by a set of Mathieu–Hill equations and, consequently, that loss of dynamic stability is to be expected for certain combinations of system parameters. Along with outward-oriented beams, inward-oriented ones are also considered for which loss of static stability (buckling) is also possible. In order to facilitate getting insight into the peculiarities of the fluctuating speed problem, certain aspects of the constant speed problem are first highlighted. Stability analysis is then performed for the fluctuating speed problem through a generalized Bolotin method given by Turhan [23] and a monodromy matrix method. Stability analysis results are presented in the form of stability charts reflecting stability's dependence on various selected pairs of system parameters.

2. Formulation of the problem

2.1. Equation of motion

The lateral vibrations of a uniform Euler–Bernouilli beam made of a Kelvin–Voigt material subjected to a distributed force whose axial and transversal components are given, respectively, as $f_x(x,t)$ and $f_y(x,t)$ can be shown to be governed by the integro-partial differential equation

$$\mathrm{EI}\frac{\partial^4}{\partial x^4}\left[y(x,t)+\eta\frac{\partial y(x,t)}{\partial t}\right]+\rho A\frac{\partial^2 y(x,t)}{\partial t^2}-\left[\int_x^{\ell} f_x(\xi,t)\,\mathrm{d}\xi\right]\frac{\partial^2 y(x,t)}{\partial x^2}+f_x(x,t)\frac{\partial y(x,t)}{\partial x}-f_y(x,t)=0, \tag{1}$$

where EI is the flexural rigidity, A the cross-section area, ρ the mass density, ℓ the length of the beam and η is a viscous damping coefficient.

Eq. (1) can be used to obtain the equation of motion of the in-plane lateral vibrations of the rotating beam of Fig. 1a. To this end, it suffices to define $f_x(x,t)$ and $f_y(x,t)$ as the inertia force

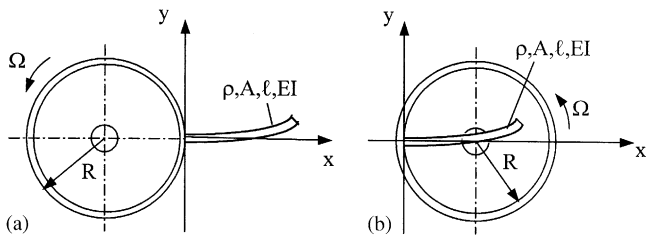

Fig. 1. Rotating beam (a: oriented outward; $\alpha \geqslant 0$, b: oriented inward; $\alpha < 0$).

components acting on a segment of unit length situated at point x of the beam, vis.

$$f_x(x,t) = \rho A\left[\Omega^2(R+x) + \frac{\mathrm{d}\Omega}{\mathrm{d}t}y(x,t) + 2\Omega\frac{\partial y(x,t)}{\partial t}\right],$$
$$f_y(x,t) = \rho A\left[\Omega^2 y(x,t) - \frac{\mathrm{d}\Omega}{\mathrm{d}t}(R+x)\right]. \tag{2}$$

This leads to

$$\begin{aligned}&\mathrm{EI}\frac{\partial^4}{\partial x^4}\left[y(x,t)+\eta\frac{\partial y(x,t)}{\partial t}\right] + \rho A\frac{\partial^2 y(x,t)}{\partial t^2} - \rho A\Omega^2\left[R(\ell-x)+\tfrac{1}{2}(\ell^2-x^2)\right]\frac{\partial^2 y(x,t)}{\partial x^2}\\ &- \rho A\left\{\int_x^\ell\left[\frac{\mathrm{d}\Omega}{\mathrm{d}t}y(\xi,t)+2\Omega\frac{\partial y(\xi,t)}{\partial t}\right]\mathrm{d}\xi\right\}\frac{\partial^2 y(x,t)}{\partial x^2} + \rho A\left[\frac{\mathrm{d}\Omega}{\mathrm{d}t}y(x,t)+2\Omega\frac{\partial y(x,t)}{\partial t}\right]\frac{\partial y(x,t)}{\partial x}\\ &+ \rho A\Omega^2(R+x)\frac{\partial y(x,t)}{\partial x} - \rho A\left[\Omega^2 y(x,t) - \frac{\mathrm{d}\Omega}{\mathrm{d}t}(R+x)\right] = 0.\end{aligned} \tag{3}$$

Now, assume that the rotation speed fluctuates sinusoidally with a frequency v about a mean value Ω_0 so that

$$\Omega(t) = \Omega_0 + \Omega_1 \sin\, vt, \tag{4}$$

neglect the nonlinear fourth and fifth terms of Eq. (3), put in non-dimensional form and obtain

$$L(v) = \ddot{v} + \frac{\zeta}{\omega}\dot{v}^{\mathrm{IV}} + \frac{1}{\omega^2}v^{\mathrm{IV}} - \frac{\beta(\tau)^2}{\omega^2}\left\{\left[\alpha(1-u)+\tfrac{1}{2}(1-u^2)\right]v'' - (\alpha+u)v' + v\right\} + \frac{\dot{\beta}(\tau)}{\omega}(\alpha+u) = 0, \tag{5}$$

where

$$\beta(\tau) = \beta_0\left(1+\frac{\delta}{2}\sin\,\tau\right) \tag{6}$$

and

$$u = \frac{x}{\ell},\quad v = \frac{y}{\ell},\quad \alpha = \frac{R}{\ell},\quad \tau = vt,\quad \omega = \frac{v}{\omega^*},\quad \zeta = \eta\omega^*,$$
$$\beta = \frac{\Omega}{\omega^*},\quad \beta_0 = \frac{\Omega_0}{\omega^*},\quad \delta = \frac{2\Omega_1}{\Omega_0},\quad \omega^* = \sqrt{\frac{\mathrm{EI}}{\rho A\ell^4}} \tag{7}$$

as the partial differential equation of motion. The accompanying boundary conditions are those of a fixed-free beam

$$v(0,\tau) = v'(0,\tau) = v''(1,\tau) = v'''(1,\tau) = 0. \tag{8}$$

In Eqs. (5) and (8) overdots denote differentiation w.r.t. τ and primes denote differentiation w.r.t. u. Eq. (5) can be used to study the vibrations of both outward and inward-oriented beams (Fig. 1a and b) by adjusting the sign of α. In the first case one has $\alpha \geqslant 0$ and in the second $\alpha < 0$. Let one also note that δ of Eq. (6) is nothing but a coefficient of fluctuation; a concept familiar to those acquainted with the problems of dynamics of machinery [24].

2.2. Galerkin discretization

The boundary-value problem defined in Eqs. (5)–(8) can be approximated by a finite set of ordinary differential equations by means of Galerkin's method. To this end, introduce the n term Galerkin series

$$\tilde{v}(u,\tau) = \sum_{i=1}^{n} g_i(\tau)\varphi_i(u), \tag{9}$$

for the nth order approximate solution, use the orthonormal set of eigenfunctions

$$\varphi_i(u) = \cosh\,\lambda_i u - \cos\,\lambda_i u - \frac{\cosh\,\lambda_i + \cos\,\lambda_i}{\sinh\,\lambda_i + \sin\,\lambda_i}(\sinh\,\lambda_i u - \sin\,\lambda_i u) \tag{10}$$

of a stationary Euler–Bernouilli beam with boundary conditions (8) as the set of comparison functions (the first five eigenvalues λ_i are given in Appendix A), substitute $\tilde{v}$ for v from Eq. (9) into Eq. (5) and orthogonalize the latter with respect to the set $\varphi_j(u)$ by requiring

$$\int_0^1 L(\tilde{v})\varphi_j(u)\,\mathrm{d}u = 0; \quad j = 1,2,\ldots,n \tag{11}$$

to obtain

$$\ddot{g}_i(\tau) + \frac{\zeta}{\omega}\lambda_i^4\dot{g}_i(\tau) + \frac{1}{\omega^2}\left\{\lambda_i^4 g_i(\tau) - \beta(\tau)^2\sum_{j=1}^{n}(\alpha A_{ij} + B_{ij} + \delta_{ij})g_j(\tau)\right\} = -\frac{\dot{\beta}(\tau)}{\omega}(\alpha c_i + d_i);$$
$$i = 1,2,\ldots,n \tag{12}$$

where

$$A_{ij} = \int_0^1 \left[(1-u)\varphi_i'' - \varphi_i'\right]\varphi_j\,\mathrm{d}u, \quad B_{ij} = \int_0^1 \left[\tfrac{1}{2}(1-u^2)\varphi_i'' - u\varphi_i'\right]\varphi_j\,\mathrm{d}u,$$
$$c_i = \int_0^1 \varphi_i\,\mathrm{d}u, \quad d_i = \int_0^1 u\varphi_i\,\mathrm{d}u, \quad \delta_{ij} = \text{Kronecker delta}. \tag{13}$$

The differential equation set (12) can conveniently be written in vector–matrix form as

$$\ddot{\mathbf{g}}(\tau) + \frac{\zeta}{\omega}\mathbf{\Lambda}^4\dot{\mathbf{g}}(\tau) + \frac{1}{\omega^2}[\mathbf{\Lambda}^4 - \beta(\tau)^2(\alpha\mathbf{A} + \mathbf{B} + \mathbf{I})]\mathbf{g}(\tau) = -\frac{\dot{\beta}(\tau)}{\omega}(\alpha\mathbf{c} + \mathbf{d}), \tag{14}$$

where **A** and **B** are $n \times n$ symmetrical matrices and **c** and **d** are n-dimensional vectors whose elements are defined in Eq. (13) and numerically given in Appendix A for $n=5$, $\mathbf{\Lambda}$ is an $n \times n$ diagonal matrix with elements $\Lambda_{ij} = \lambda_i \delta_{ij}$, **I** is the $n \times n$ unit matrix, and $\mathbf{g}(\tau)$ is an n dimensional vector of unknowns with elements $g_i(\tau)$.

Eq. (14) constitutes a system of linear ordinary differential equations with 2π periodic coefficients, or, a system of Mathieu–Hill equations.

3. A review of the constant speed problem

Before embarking upon the study of the fluctuating speed problem, a brief review of the undamped, constant speed problem will prove to be helpful. To this end put $\zeta = 0$, $\delta = 0$ and $\omega = 1$ in Eq. (14) to obtain

$$\ddot{\mathbf{g}}(\tau) + [\mathbf{\Lambda}^4 - \beta_0^2(\alpha\mathbf{A} + \mathbf{B} + \mathbf{I})]\mathbf{g}(\tau) = \mathbf{0} \tag{15}$$

as an approximate discretized mathematical model for the vibrations of a beam rotating at a constant dimensionless rate β_0.

3.1. Natural frequencies

Requiring Eq. (15) to have a solution in the form $\mathbf{g}(\tau) = \mathbf{G}e^{i\mu^2\tau}$ (harmonic in time) where **G** is an n-dimensional unknown amplitudes' vector, one is led to the eigenvalue analysis problem

$$\det[\mathbf{\Lambda}^4 - \beta_0^2(\alpha\mathbf{A} + \mathbf{B} + \mathbf{I}) - \mu^4\mathbf{I}] = 0 \tag{16}$$

the solution of which gives the dimensionless natural frequencies μ_i of the rotating beam. The radial natural frequencies ω_i are then calculated from

$$\omega_i = \mu_i^2 \omega^*, \quad i = 1, 2, \ldots, n, \tag{17}$$

where ω^* is as given in Eq. (7). Fig. 2 shows the variation of the first four eigenvalues μ_i with β_0 for various values of the offset ratio α, as calculated from Eq. (16) with $n=10$. Fig. 2 (and also Eq. (16)) shows that $\mu_i = \lambda_i$ for $\beta_0 = 0$, as it should. As can be seen in this figure, all the eigenvalues of the outward-oriented beam ($\alpha \geqslant 0$) increase with both β_0 and α, this obviously being due to the tensile and restoring effect of the centrifugal forces. But the situation is not that clear for the inward-oriented beam ($\alpha < 0$) for which compressive and destabilizing effects of the centrifugal forces come in to play. In this case, eigenvalues may increase or decrease with increasing β_0, depending on the value of α and also on the considered range of β_0. A decreasing eigenvalue vanishes at a certain critical combination of the parameters β_0 and α, beyond which loss of static stability (buckling) occurs in the corresponding mode.

3.2. Buckling of inward-oriented beams

The line separating the statically stable and unstable (buckling) regions on a $\beta_0 - \alpha$ plane can be obtained from Eq. (16) by putting $\mu = 0$ and recasting the resulting problem into the form of an

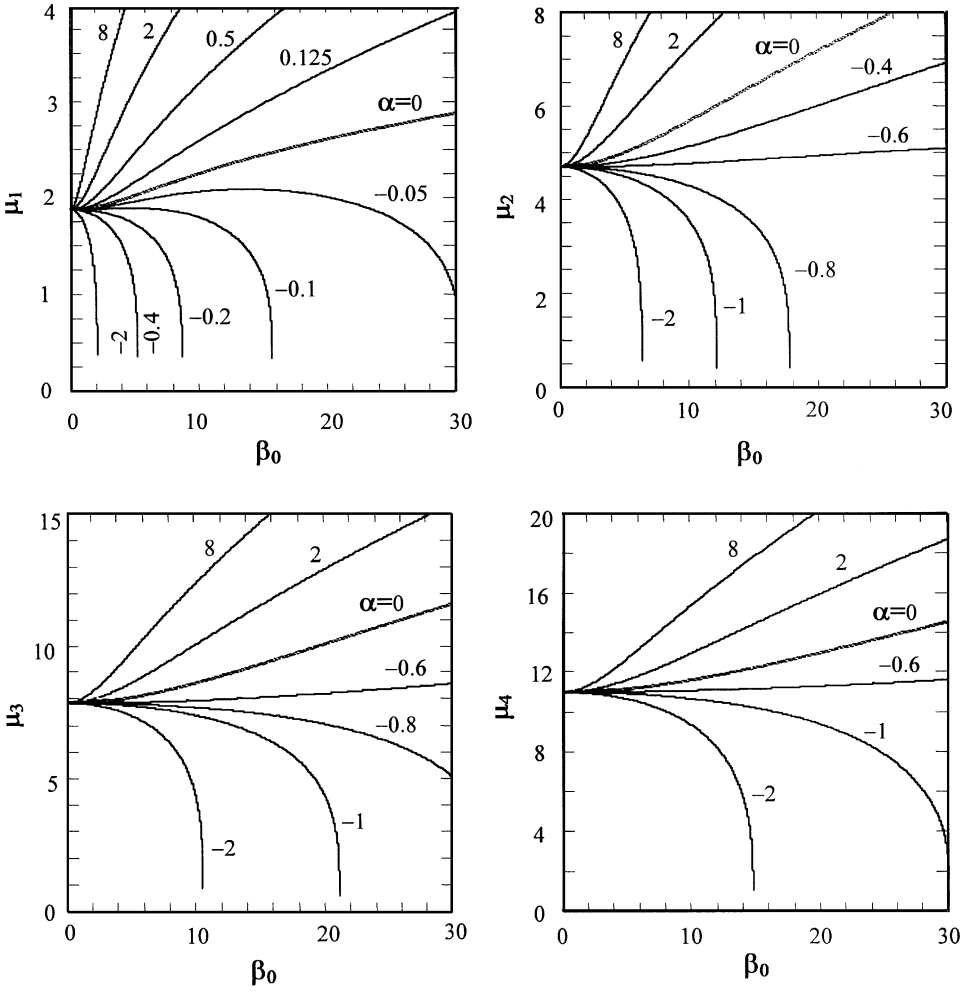

Fig. 2. Variation of the first four eigenfrequencies with the rotation speed.

eigenvalue analysis problem giving α in terms of β_0^2 as

$$\det\left[\mathbf{A}^{-1}\left(\frac{1}{\beta_0^2}\mathbf{\Lambda}^4 - \mathbf{B} - \mathbf{I}\right) - \alpha\mathbf{I}\right] = 0 \tag{18}$$

or, alternatively, an eigenvalue analysis problem giving β_0^2 in terms of α as

$$\det[(\alpha\mathbf{A} + \mathbf{B} + \mathbf{I})^{-1}\mathbf{\Lambda}^4 - \beta_0^2\mathbf{I}] = 0. \tag{19}$$

Fig. 3a shows buckling limits (lower boundaries of statically unstable parameter regions) of the first seven modes and Fig. 3b that of the first mode alone, as calculated from Eq. (18) with $n = 10$. It is possible to obtain a closed form approximate expression for the first mode buckling limit

from Eq. (18) or (19) with $n=2$. Using the latter one has

$$\beta_0(\alpha) = 5.695145\sqrt{-\frac{\alpha + 0.185826 + 0.757884\sqrt{\alpha^2 + 0.110970\alpha + 0.027575}}{\alpha^2 + 0.723457\alpha + 0.043919}}. \tag{20}$$

A literature survey revealed a number of similar formulae, their performance is compared [25], and the best is found to be the below-reproduced formula due to Peters and Hodges [20]

$$\alpha(\beta_0) = -\left[\frac{2\sqrt{2}}{\pi\beta_0}\operatorname{arctg}\left(\frac{0.1319937523\pi\beta_0}{2\sqrt{2}}\right) + \frac{7.8373474390}{\beta_0^2}\right]. \tag{21}$$

Eqs. (20) and (21) are also plotted in Fig. 3b but the plot of Eq. (21) is not visible as it superimposes with that of Eq. (18) with $n=10$.

3.3. Tuning

As the natural frequencies of the rotating beam depend on the parameters β_0 and α, parameter combinations may arise for which $\Omega_0 = \omega_i$; $i = 1, 2, \ldots$, where Ω_0 is the shaft velocity and ω_i is the ith radial frequency of the beam defined in Eq. (17). This phenomenon is called tuning. Tuning is important because when it is present, any periodic forcing effect due to the rotation of the shaft will be resonant. To obtain tuning conditions put $\mu^4 = \beta_0^2$ into Eq. (16) and recast the resulting problem into the form of an eigenvalue analysis problem giving α in terms of β_0 as

$$\det\left[\mathbf{A}^{-1}\left(\frac{1}{\beta_0^2}\mathbf{\Lambda}^4 - \mathbf{B} - 2\mathbf{I}\right) - \alpha\mathbf{I}\right] = 0 \tag{22}$$

or, alternatively, an eigenvalue analysis problem giving β_0 in terms of α as

$$\det[(\alpha\mathbf{A} + \mathbf{B} + 2\mathbf{I})^{-1}\mathbf{\Lambda}^4 - \beta_0^2\mathbf{I}] = 0. \tag{23}$$

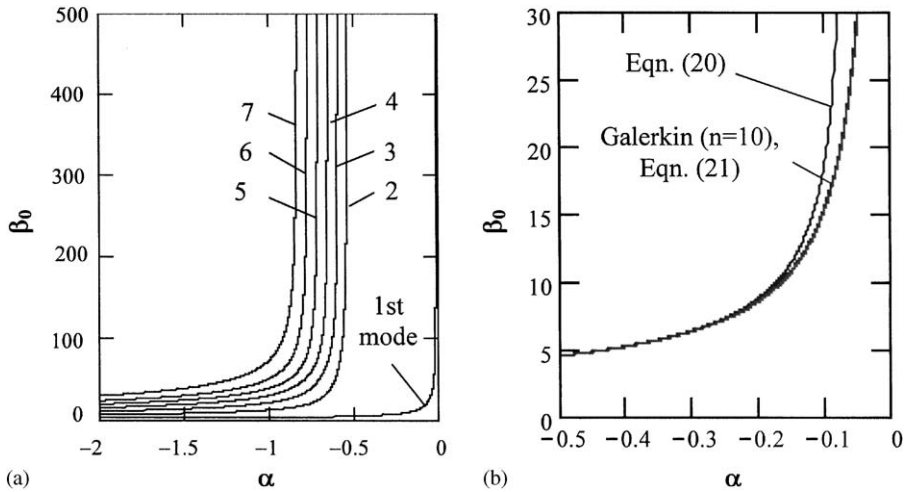

Fig. 3. Static stability (buckling) boundaries for inward-oriented beam (a, first 7 modes; b, first mode).

A closed form approximate expression for the locus of the parameter combinations for which first mode's tuning occurs can be obtained from, say, Eq. (22) with $n=2$. This yields

$$\alpha(\beta_0) = 0.019391 - \frac{32.434674 - 24.581725\sqrt{1 + 0.039434\beta_0^2 + 0.000505\beta_0^4}}{\beta_0^2}. \tag{24}$$

Fig. 4 shows tuning conditions for the first three modes as obtained from Eq. (22) with $n=10$, and along with, the results of Eq. (24). It can be seen in this figure that tuning of the first mode is always possible for inward-oriented ($\alpha<0$) beams, and up to a certain value of α for outward-oriented ($\alpha\geqslant 0$) ones (an estimate for this value is $\alpha\approx 0.6554$ according to Eq. (22) with $n=10$ and $\beta_0\to\infty$, see also Ref. [14]).

Unlike the natural frequencies calculation and buckling problems, which will prove to be helpful in getting insight into some peculiarities of the dynamic stability analysis problem of fluctuating speed beams, the tuning problem will not need to be referenced further. It is included here only for the purpose of completing the panorama of the constant speed problems.

4. Dynamic stability analysis

Systems whose dynamic behavior is governed by Mathieu–Hill equations such as Eq. (14) are referred to as parametrically excited systems and, as such, are subject to special resonance conditions peculiar to them. The determination problem of these conditions is called dynamic stability analysis and requires the homogeneous part of the equation to be considered. Thus consider

$$\ddot{\mathbf{g}}(\tau) + \frac{\zeta}{\omega}\mathbf{\Lambda}^4\dot{\mathbf{g}}(\tau) + \frac{1}{\omega^2}\left[\mathbf{\Lambda}^4 - \beta(\tau)^2(\alpha\mathbf{A} + \mathbf{B} + \mathbf{I})\right]\mathbf{g}(\tau) = \mathbf{0}. \tag{25}$$

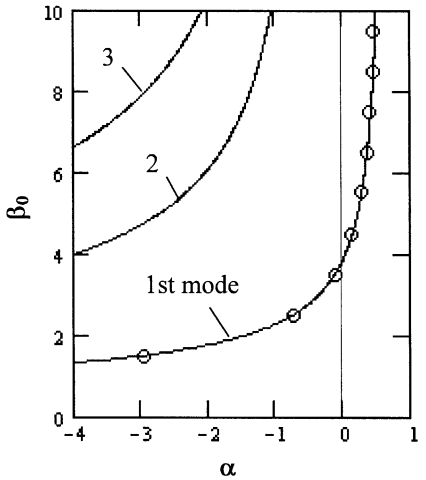

Fig. 4. Tuning of the first three modes (o o o, Eq. (24)).

Stability of the solutions of Eq. (25) will be studied via two alternative methods. These methods are briefly described below.

4.1. The monodromy matrix method

A state-space representation of system (25) may be given as

$$\dot{\mathbf{u}} = \mathbf{H}(\zeta, \omega, \beta_0, \delta, \alpha; \tau)\mathbf{u}, \quad \mathbf{H}(\zeta, \omega, \beta_0, \delta, \alpha; \tau) = \mathbf{H}(\zeta, \omega, \beta_0, \delta, \alpha; \tau + 2\pi), \tag{26}$$

where $\mathbf{u}$ is a $2n$-dimensional vector defined as $\mathbf{u}(\tau) = \{\, \mathbf{g}(\tau) \quad \dot{\mathbf{g}}(\tau) \,\}^{\mathrm{T}}$ and $\mathbf{H}$ is a $2n \times 2n$-dimensional matrix defined as

$$\mathbf{H}(\zeta, \omega, \beta_0, \delta, \alpha; \tau) = \begin{bmatrix} \mathbf{0} & \mathbf{I} \\ -\frac{1}{\omega^2}\left[\mathbf{\Lambda}^4 - \beta(\tau)^2(\alpha\mathbf{A} + \mathrm{B} + \mathrm{I})\right] & -\frac{\zeta}{\omega}\mathbf{\Lambda}^4 \end{bmatrix}. \tag{27}$$

According to the Floquet theory [26], a fundamental solutions' matrix of system (26) can be expressed as

$$\mathbf{\Phi}(\tau) = Q(\tau)\mathrm{e}^{\mathbf{R}\tau}, \tag{28}$$

where $\mathbf{Q}(\tau)$ is a 2π periodic matrix and $\mathbf{R}$ is a $2n \times 2n$ constant matrix. It then follows that $\mathbf{\Phi}(\tau_0 + 2\pi) = \mathbf{\Phi}(\tau_0)\mathbf{S}$ with $(1/2\pi)\ln \mathbf{S} = \mathbf{R}$. If the fundamental matrix is normalized so that $\mathbf{\Phi}(\tau_0) = \mathbf{I}$ the $2n \times 2n$ constant matrix $\mathbf{S}$ is simply

$$\mathbf{S} = \mathbf{\Phi}(\tau_0 + 2\pi). \tag{29}$$

The matrix $\mathbf{S}$, which is nothing but a period-advance mapping, is referred to as a monodromy matrix. Its eigenvalues σ_i; $i = 1, 2, \ldots, 2n$ called the Floquet multipliers govern the stability of the system so that the system is stable (non-resonant) if and only if $\mathrm{mod}(\sigma_i) \leqslant 1$ for all i (where the equal sign holds only when the multiplicity of σ_i equals it s nullity).

The monodromy matrix method consists of obtaining the matrix $\mathbf{S}$ of Eq. (29) by a $2n$ passes numerical integration of Eq. (26) and looking up its eigenvalues to assess stability of the system. As the problem depends on the parameters ζ, ω, β_0, δ and α, the method may be used as a scatter plot method for obtaining stability charts on a plane having a selected couple of these parameters as its components.

4.2. The generalized Bolotin method

Unlike the monodromy matrix method that is a scatter plot method; this method is a boundary tracing method for obtaining stability charts on a two-dimensional parameter plane having the dimensionless parametric frequency ω as one of its components. The method is described in Ref. [23] and will be summarized below. Eq. (25) may be written

$$\ddot{\mathbf{g}}(\tau) + \frac{1}{\omega}\mathbf{Q}\dot{\mathbf{g}}(\tau) + \frac{1}{\omega^2}\mathbf{S}(\tau)\mathbf{g}(\tau) = \mathbf{0}, \tag{30}$$

where

$$\mathbf{Q} = \zeta\mathbf{\Lambda}^4, \quad \mathbf{S}(\tau) = \mathbf{\Lambda}^4 - \beta(\tau)^2(\alpha\mathbf{A} + \mathbf{B} + \mathbf{I}). \tag{31}$$

Now, assume a single solution of form (28)

$$\mathbf{g}(\tau) = \mathrm{e}^{\rho\tau} \sum_{k=-\infty}^{\infty} \mathbf{D}_k \mathrm{e}^{\mathrm{i}k\tau}, \tag{32}$$

where ρ (a Floquet exponent) corresponds to an eigenvalue of the matrix $\mathbf{R}$ and the periodic part of the solution is represented by a complex Fourier series with unknown coefficient vectors $\mathbf{D}_k$, represent the 2π periodic matrix $\mathbf{S}(\tau)$ by its complex Fourier series expansion,

$$\mathbf{S}(\tau) = \sum_{p=-2}^{2} \mathbf{S}_p \mathrm{e}^{\mathrm{i}p\tau} \tag{33}$$

where the complex Fourier coefficient matrices $\mathbf{S}_p$; $p = -2, -1, 0, 1, 2$ are easily obtained by substituting the exact expansion

$$\beta(\tau)^2 = \beta_0^2 \left[\left(1 + \frac{\delta^2}{8} \right) + \mathrm{i}\frac{\delta}{2}(\mathrm{e}^{\mathrm{i}\tau} - \mathrm{e}^{-\mathrm{i}\tau}) - \frac{\delta}{16}(\mathrm{e}^{\mathrm{i}2\tau} + \mathrm{e}^{-\mathrm{i}2\tau}) \right] \tag{34}$$

into Eq. (31), insert Eqs. (32) and (33) into Eq. (30) and collect equal powers of $\mathrm{e}^{\mathrm{i}\tau}$ to obtain

$$(\rho + \mathrm{i}k)\left[(\rho + \mathrm{i}k)\mathbf{I} + \frac{1}{\omega}\mathbf{Q} \right] \mathrm{D}_k + \frac{1}{\omega^2} \sum_{p=-2}^{2} \mathbf{S}_p \mathbf{D}_q = \mathbf{0}, \quad k = \ldots, -2, -1, 0, 1, 2, \ldots, q = k - p. \tag{35}$$

Eq. (35) constitutes an infinite system of homogeneous algebraic equations for the unknown vectors $\mathbf{D}_k$. This system may conveniently be written in a hyper-matrix/vector form as

$$\left[\rho^2 \mathbf{I} + \rho \left(\mathbf{E}_0 + \frac{1}{\omega}\mathbf{E} \right) + \left(\mathbf{F}_0 + \frac{1}{\omega}\mathbf{F}_1 + \frac{1}{\omega^2}\mathbf{F}_2 \right) \right] \mathbf{D} = \mathbf{0}, \tag{36}$$

where $\mathbf{D}$ is an infinite hyper-vector defined as $D = \{\ldots, \mathbf{D}_{-2}^{\mathrm{T}}, \mathbf{D}_{-1}^{\mathrm{T}}, \mathbf{D}_0^{\mathrm{T}}, \mathbf{D}_1^{\mathrm{T}}, \mathbf{D}_2^{\mathrm{T}}, \ldots\}^{\mathrm{T}}$, $\mathbf{I}$ is the infinite dimensional unit matrix and $\mathbf{E}_i$, $\mathbf{F}_i$'s are infinite dimensional hyper-matrices made up of $2n \times 2n$ sub-matrices given by

$$\mathbf{E}_0^{k,q} = 2\mathrm{i}k\mathbf{I}\delta_{kq}, \quad \mathbf{E}_1^{k,q} = \mathbf{Q}\delta_{kq}, \quad \mathbf{F}_0^{k,q} = -k^2\mathbf{I}\delta_{kq}, \quad \mathbf{F}_1^{k,q} = \mathrm{i}k\mathbf{Q}\delta_{kq}, \quad \mathbf{F}_2^{k,q} = \mathbf{S}_p, \tag{37}$$

where δ_{kq} is the Kronecker delta and the superscripts k and q refer to the hyper-row and column indices. In order Eq. (30) to admit a non-trivial solution of form (32), the determinant of the coefficients' matrix of Eq. (36) must vanish

$$\det\left[\rho^2 \mathbf{I} + \rho \left(\mathbf{E}_0 + \frac{1}{\omega}\mathbf{E}_1 \right) + \left(\mathbf{F}_0 + \frac{1}{\omega}\mathbf{F}_1 + \frac{1}{\omega^2}\mathbf{F}_2 \right) \right] = 0. \tag{38}$$

This equation can be used to calculate the ω values corresponding to stability boundaries provided that the value of the Floquet exponent ρ on those boundaries is known. It is customary to differentiate between three kinds of resonances and thereof of stability boundaries. These are harmonic, sub-harmonic and combination resonances. It is known that on harmonic and sub-harmonic resonance boundaries a certain sth exponent takes, respectively, the values $\rho_s = 0$ and $\rho_s = \mathrm{i}/2$, while for a non-canonical system such as the one considered here, on a combination resonance boundary a certain pair (ρ_s, ρ_t); $s \neq t$ of Floquet exponents take values so that $\rho_s + \rho_t = 0$ [23]. Whence, substituting $\rho = 0$ into Eq. (38), one has for harmonic parametric resonance

boundaries

$$\det\left[\mathbf{F}_0+\frac{1}{\omega}\mathbf{F}_1+\frac{1}{\omega^2}\mathbf{F}_2\right]=0 \tag{39}$$

and substituting $\rho=\mathrm{i}/2$ one has for sub-harmonic parametric resonance boundaries

$$\det\left[\left[\mathbf{F}_0+\frac{\mathrm{i}}{2}\mathbf{E}_0-\frac{1}{4}\mathbf{I}\right]+\frac{1}{\omega}\left[\mathbf{F}_1+\frac{\mathrm{i}}{2}\mathbf{E}_1\right]+\frac{1}{\omega^2}\mathbf{F}_2\right]=0, \tag{40}$$

while for combination resonance boundaries, first linearize the matrix polynomial of Eq. (38), which is a monic matrix polynomial of second degree in ρ, to obtain the Hill's determinant of the problem

$$\det\left[\left[\mathbf{U}_0+\frac{1}{\omega}\mathbf{U}_1+\frac{1}{\omega^2}\mathbf{U}_2\right]-\rho\mathbf{I}\right]=0, \tag{41}$$

where

$$\mathbf{U}_0=\begin{bmatrix}-\mathbf{E}_0 & -\mathrm{F}_0\\ \mathbf{I} & \mathbf{0}\end{bmatrix},\quad \mathbf{U}_1=\begin{bmatrix}-\mathbf{E}_1 & -\mathbf{F}_1\\ \mathbf{0} & \mathbf{0}\end{bmatrix},\quad \mathbf{U}_2=\begin{bmatrix}\mathbf{0} & -\mathbf{F}_2\\ \mathbf{0} & \mathbf{0}\end{bmatrix}. \tag{42}$$

Then introduce the bialternate sum matrices $\mathbf{B}(\mathbf{U}_i)$of the matrices $\mathbf{U}_i$, which have the property of having as eigenvalues, the sums of the eigenvalues of the argument matrix taken in pairs [27] (see Ref. [27] or [23] for the construction of these matrices) and write as a condition for $\rho_s+\rho_t=0$,

$$\det\left[\mathbf{B}(\mathbf{U}_0)+\frac{1}{\omega}\mathbf{B}(\mathbf{U}_1)+\frac{1}{\omega^2}\mathbf{B}(\mathbf{U}_2)\right]=0 \tag{43}$$

for combination resonance boundaries. ω values corresponding to stability boundaries can be calculated from Eqs. (39), (40) and (43) by solving an eigenvalue analysis problem. To this end, note that all the three equations are of the form

$$\det\left[\mathbf{M}_0+\frac{1}{\omega}\mathbf{M}_1+\frac{1}{\omega^2}\mathbf{M}_2\right]=0 \tag{44}$$

thus, involving matrix polynomials of second degree in $1/\omega$. Multiplying by ω^2 and linearizing, one may write

$$\det\left[\begin{bmatrix}-\mathbf{M}_0^{-1}\mathbf{M}_1 & -\mathbf{M}_0^{-1}\mathbf{M}_2\\ \mathbf{I} & \mathbf{0}\end{bmatrix}-\omega\mathbf{I}\right]=0 \tag{45}$$

whenever $\mathbf{M}_0$ is invertible. When this is not the case, first put $1/\omega=1/\bar{\omega}+1/\delta$ (where $1/\delta$ is a scalar not equalling a proper value of the matrix polynomial in question) into Eq. (43) and solve Eq. (44) with

$$\bar{\mathbf{M}}_0=\mathbf{M}_0+\frac{1}{\delta}\mathbf{M}_1+\frac{1}{\delta^2}\mathbf{M}_2,\quad \bar{\mathbf{M}}_1=\mathbf{M}_1+\frac{1}{2\delta}\mathbf{M}_2,\quad \bar{\mathbf{M}}_2=\mathbf{M}_2 \tag{46}$$

for $\bar{\omega}$, and then calculate ω as $\omega=\delta\bar{\omega}/(\delta+\bar{\omega})$.

As a note on the implementation of the above-described method, it should be noted that all the ω values calculated through Eqs. (39), (40) and (43) are not admissible. One has to eliminate those ω values that are not real numbers, and those corresponding to unconverged (ρ_s, ρ_t) pairs or to pairs whose imaginary parts violate the inequality $-\frac{1}{2}<\mathrm{Im}(\rho_{s,t})<\frac{1}{2}$. The first condition that follows from obvious physical considerations applies to any of problems (39), (40) and (43), and is implemented with no additional effort. But the second condition that is ultimately related to the redundant and periodic (i periodic in ρ) nature of the Hill's determinant of Eq. (41) applies only to problem (43) and its implementation requires the corresponding ρ values to be calculated through Eq. (41).

5. Numerical examples

This section is devoted to dynamic stability analysis examples. The results will be presented in the form of stability charts constructed on various parameter planes. The $\omega-\beta_0$, $\omega-\alpha$ and $\omega-\delta$ planes will be considered for this purpose so as to give an idea on the effect of these four system parameters on the stability. In all of the numerical examples the only remaining system parameter ζ will be set to $\zeta = 0.0001$. Thus, almost undamped systems will be considered. Each stability chart will be worked out twice; once using the generalized Bolotin method, and once the monodromy matrix method. This will provide a verification of the results obtained and will enable us to compare the faculties of the considered methods. In the generalized Bolotin method, the matrix dimensions depend on the number n of the considered terms in the Galerkin series of Eq. (9) and the truncation number K of the Fourier series of Eq. (32). These dimensions are $\eta_1 = 2n(2K+1)$ for the determination problems of harmonic and sub-harmonic parametric resonance boundaries (Eqs. (39) and (40)) and $\eta_2 = \eta_1(\eta_1 - 1)$ for that of combination resonance boundaries (Eq. (43)). In the numerical examples $n=5$, $K=10$ ($\eta_1 = 210$) are taken in problems (39) and (40) and $n=3$, $K=3$ ($\eta_2 = 1722$) in problem (43). The method is implemented by using a special FORTRAN code developed for this purpose. On the other hand, in the monodromy matrix method, the numerical burden depends directly on n. This value is set to $n=3$ in the numerical examples and the method is implemented by using the MATLAB package.

Before proceeding to the presentation of the obtained stability charts, a discussion on their expected features will be in order. It is known that the locations of the unstable parameter zones (resonance regions) on these charts depend on the natural frequencies of the system. Specifically, if the ω-axis corresponds to vanishing parametric excitation and if no damping is present, the so-called kth order harmonic and sub-harmonic parametric resonance regions related to the ith vibration mode will emanate from, respectively, the points

$$\omega_{ik}^{H} = \frac{\mu_i^2}{k}, \quad \omega_{ik}^{S} = \frac{2\mu_i^2}{(2k-1)}, \quad k = 1, 2, \ldots \tag{47}$$

of the ω-axis while the kth order sum or difference type combination resonance regions of the ith and jth modes emanating from

$$\omega_{ijk}^{C\pm} = \frac{\mu_j^2 \pm \mu_i^2}{k}, \quad j > i. \tag{48}$$

But for the considered rotating beam problem, it is known from the content of Section 3.1 that in the constant speed case the dimensionless natural frequencies of the system depend on the dimensionless eccentricity α and the square of the dimensionless rotation speed β_0 (see Eq. (16)). Furthermore, it is clear from Eq. (34) that, in the fluctuating speed case the effective average squared speed is

$$\beta_{0_{\text{eff}}}^2 = \beta_0^2\left(1+\frac{\delta^2}{8}\right). \tag{49}$$

Thus, one concludes that the natural frequencies of the fluctuating speed system will be $\mu_i = \mu_i(\alpha, \beta_0, \delta)$, that is, they will depend on α, β_0 and δ and therefore so will the locations of the resonance regions.

On the other hand, it is known from the content of Section 3.2 that an inward-oriented beam may suffer loss of static stability for certain combinations of the system parameters and that the boundaries delimiting the unstable parameter region can be calculated, for the constant speed case, from an equation relating α to the square of the rotation speed (see Eqs. (18) and (19)). In view of Eq. (49) one concludes that, in the fluctuating speed case this equation should be understood as $f(\alpha, \beta_0, \delta) = 0$. Whether a so calculated statically unstable zone will subsist or not in the fluctuating speed case is an interesting question to be considered in a sequel.

As a first example, the stability of an inward-oriented beam with $\alpha = -0.4$, $\delta = 0.5$ (an exaggerated speed fluctuation) and $\zeta = 0.0001$ is considered and the results are presented in the form of stability charts constructed on the $\omega - \beta_0$ parameter plane in Figs. 5a–c. The chart of Fig. 5a is obtained by using the generalized Bolotin method and that of Fig. 5c by using the monodromy matrix method. Fig. 5b is simply a blow-up from Fig. 5a. Fig. 5d, on the other hand, presents some results obtained from undamped, constant speed analysis. Plotted on this figure are some functions of the squared dimensionless natural frequencies μ_i, which, according to Eqs. (47) and (48) are expected to locate the first order resonance regions related to the first two modes, and the static buckling limit of the first mode. The functions related to the natural frequencies are calculated from Eq. (16) with $n = 10$ where $\beta_{0_{\text{eff}}}^2$ is substituted from Eq. (49) for β_0^2. The static stability limit is calculated from Eq. (19) with $n = 10$ where again $\beta_{0_{\text{eff}}}^2$ is substituted for β_0^2. The so-calculated critical value of β_0 is $\beta_0 = 5.163$. (Note that Eq. (20) could also be used for this purpose. The equation would give $\beta_{0_{\text{eff}}}^2 = 5.249$ and using Eq. (49) one would obtain $\beta_0 = 5.169$.)

An inspection of these figures leads to the following conclusions: (i) Results of the two stability analysis methods compare well to each other. The obtained results are therefore reliable. The monodromy matrix method is simple and straightforward but as it has to check all the surface of the parameter plane point by point through a grid-like procedure it is very time consuming. This is especially true in the cases where narrow regions exist making it necessary for high-frequency grids to be used. On the other hand, the generalized Bolotin method has the advantage of stepping only one axis of the parameter plane and is very quick in solving problems (39) and (40) but the elimination procedure involved in problem (43) is time consuming and its programming requires experience. Let one note that, in generating the stability charts with the monodromy matrix method, the authors often had to refer to the results of the generalized Bolotin method to capture the narrow bands of instability. (ii) The results imported from constant speed analysis and given in Fig. 5d are very instructive. It can be seen that the plotted frequency functions not only point to the emanation points of the related resonance zones but also determine their paths. Furthermore,

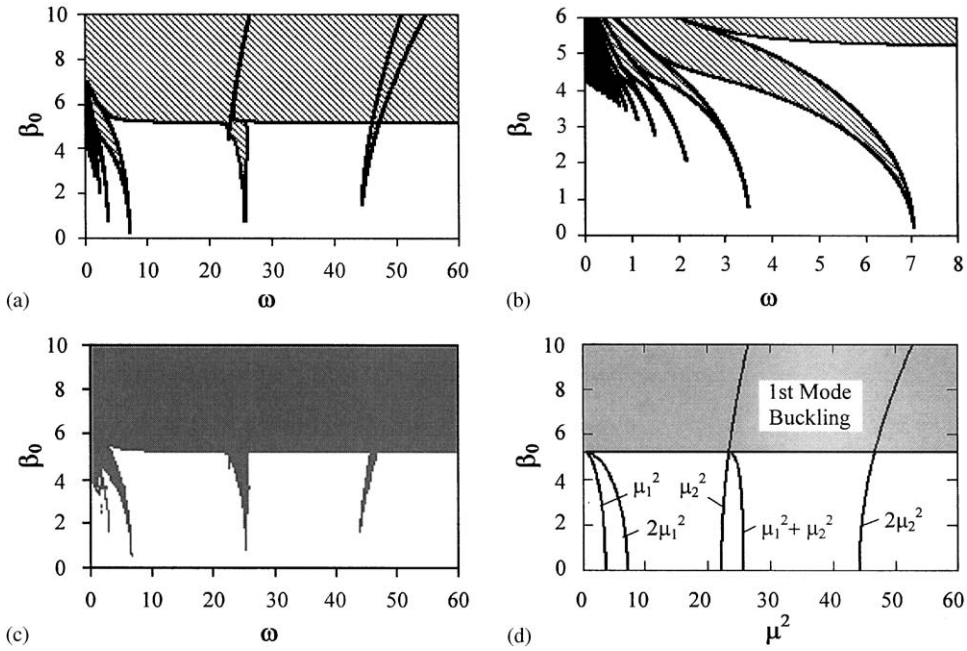

Fig. 5. Dynamic stability analysis: effect of rotation speed, inward-oriented beam; $\alpha = -0.4$, $\delta = 0.5$ (a, b, generalized Bolotin method; c, monodromy matrix method; d, results from constant speed analysis).

the static buckling region of this figure also subsists in the stability charts with only small differences. These features make of this figure something more than it is; it can be viewed as the skeleton of a dynamic stability chart. (iii) The differences of the static buckling zone appearing on Figs. 5a and c from that of Fig. 5d are such that some parameter regions that would be unstable in the absence of parametric excitation have become stable in its presence. Such a region is visible, for example, in the range $3<\omega<10$. This points to a stabilizing effect of the parametric excitation as encountered in the well-known example of the inverted pendulum. On the other hand, a number of resonance regions are visible in Figs. 5a and c. The most pronounced ones are those emanating from ω_{11}^{S}, ω_{21}^{S} and ω_{121}^{C+} (see Eqs. (47) and (48)). Notice that no difference type combination resonance region is obtained in this problem. An inspection of Fig. 5b shows that the ω_{11}^{H} region and higher order harmonic and sub-harmonic parametric resonance regions do also exist and form a sequence of gradually diminishing width zones.

The next example considers the stability of an outward-oriented beam with $\alpha = 0.4$, $\delta = 0.5$ and $\zeta = 0.0001$. Figs. 6a and b present stability charts obtained via, respectively, the generalized Bolotin method and the monodromy matrix method and Fig. 6c presents the results obtained from undamped, constant speed analysis. These results will not be elaborated on here because almost all of the comments about those of the above example also hold for the present example. An obvious exception is that loss of static stability is not in question for the present beam, which is oriented outward.

Third, the authors consider the stability of a beam with $\beta_0 = 4$ (a speed higher than the fundamental frequency of the stationary beam), $\delta = 0.5$ and $\zeta = 0.0001$ and give stability charts

constructed on the $\omega-\alpha$ parameter plane in Figs. 7a–c. Fig. 7d presents the results obtained from constant speed analysis. The charts of Figs. 7a and b are obtained via the generalized Bolotin method and that of Fig. 7c via the monodromy matrix method. As a negative α value corresponds to an inward–oriented beam, loss of static stability is expected to occur below a certain critical value of α in the range $\alpha<0$. This value is calculated from Eq. (18), with $n=10$ and where $\beta^2_{0_{\text{eff}}}$ is substituted from Eq. (49) for β^2_0, to be $\alpha=-0.596$. (Note that one could also use Eq. (21) to obtain $\alpha=-0.594$.) The corresponding buckling zone is shown in Fig. 7d where certain frequency curves are also plotted as calculated from Eq. (16) with $n=10$ and where $\beta^2_{0_{\text{eff}}}$ is substituted for β^2_0. Again a detailed discussion on the obtained results is omitted because this would be to a large extent a repetition of that given for the first example, but it is reiterated that the most pronounced instability zones are those emanating from ω^S_{11}, ω^S_{21} and ω^{C+}_{121}, and a stabilizing effect of the parametric excitation is visible in the range $3<\omega<10$.

The fourth example considers the stability of an inward-oriented beam with $\alpha=-0.4$, $\beta_0=5$, and $\zeta=0.0001$. The results are presented in the form of stability charts constructed on the $\omega-\delta$ parameter plane in Figs. 8a–c, and some results imported from constant speed analysis are

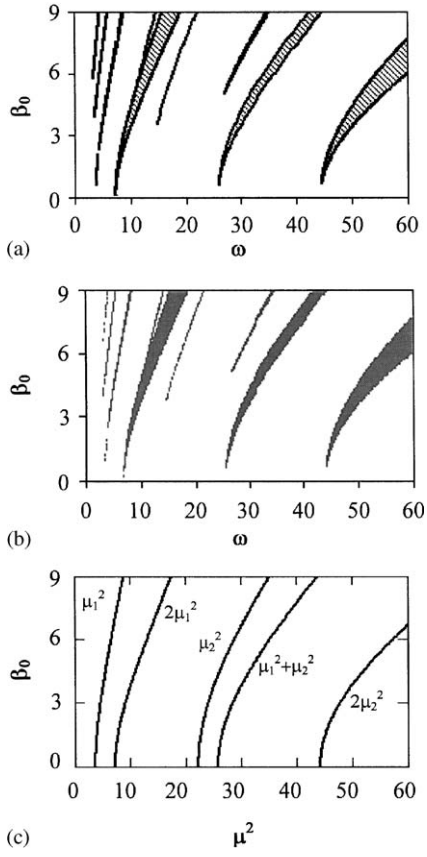

Fig. 6. Dynamic stability analysis: effect of rotation speed, outward-oriented beam; $\alpha=0.4$, $\delta=0.5$ (a, generalized Bolotin method; b, monodromy matrix method; c, results from constant speed analysis).

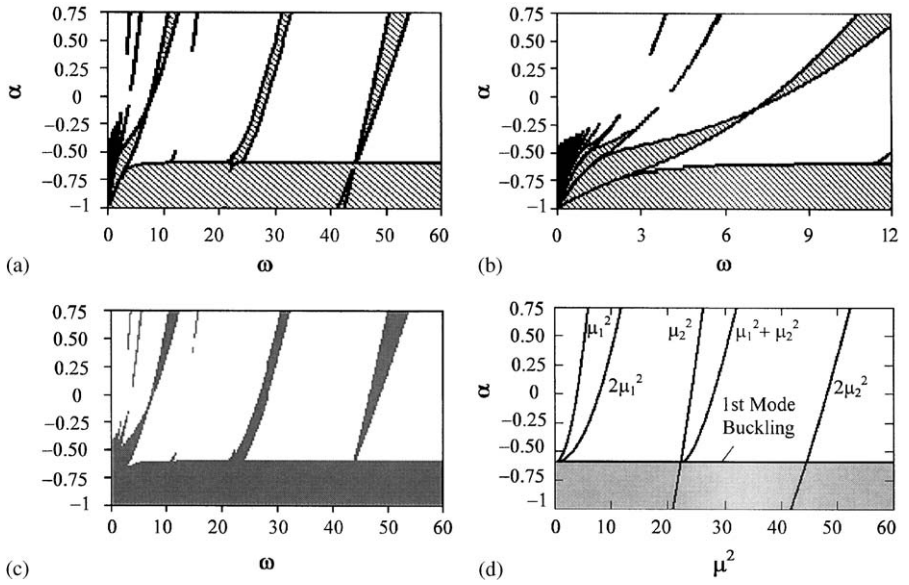

Fig. 7. Dynamic stability analysis: effect of eccentricity; $\beta_0 = 4$, $\delta = 0.5$ (a, b, generalized Bolotin method; c, monodromy matrix method; d, results from constant speed analysis).

presented in Fig. 8d. To obtain the buckling limit appearing in Fig. 8d, first $\beta^2_{0_{\text{eff}}}$ is calculated from Eq. (19) with $n=10$ to be $\beta^2_{0_{\text{eff}}} = 27.490$ and then δ is calculated from Eq. (49) as $\delta = (8(\beta^2_{0_{\text{eff}}}/\beta^2_0 - 1))^{1/2} = 0.893$. (Note that a similar calculation using Eq. (20) instead of Eq. (19) gives the same result for δ.) The most important features of the obtained figures may be summarized as follows: (i) The stabilizing effect of the parametric excitation is very clearly observed in this example, especially in the vicinity of $\omega = 6$. (ii) A larger range of ω is considered in this example, and as a result, the fundamental sum type 1–3 combination resonance region ω^{C+}_{131} has also appeared on the stability charts. It is seen that this zone is a pronounced one like ω^S_{11}, ω^S_{21} and ω^{C+}_{121} zones.

As a last example, an outward-oriented beam with $\alpha = 0.4$, $\beta_0 = 5$, and $\zeta = 0.0001$ is considered and the results are presented in Figs. 9a–c. An inspection of these figures shows that along with the bold instability zones ω^S_{11}, ω^S_{21} and ω^{C+}_{121}, the zone ω^{C+}_{131} is also partially visible at the right-hand side of the Figs. 9a and b. Also, a number of higher order resonance zones are spread out throughout the considered parameter plane.

Before closing this section, a few words about the parameter values used in the numerical examples will be in order. In all the numerical examples exceptionally high values are set to at least one of the parameters β_0 and δ. This enabled highlighting of the essential features of the dynamic stability analysis problem of rotating beams with fluctuating speed. Numerical experiments have shown that when both the dimensionless rotation speed β_0 and the speed fluctuation factor δ are realistically low, all the dynamic instability zones reduce to very narrow bands or disappear at all.

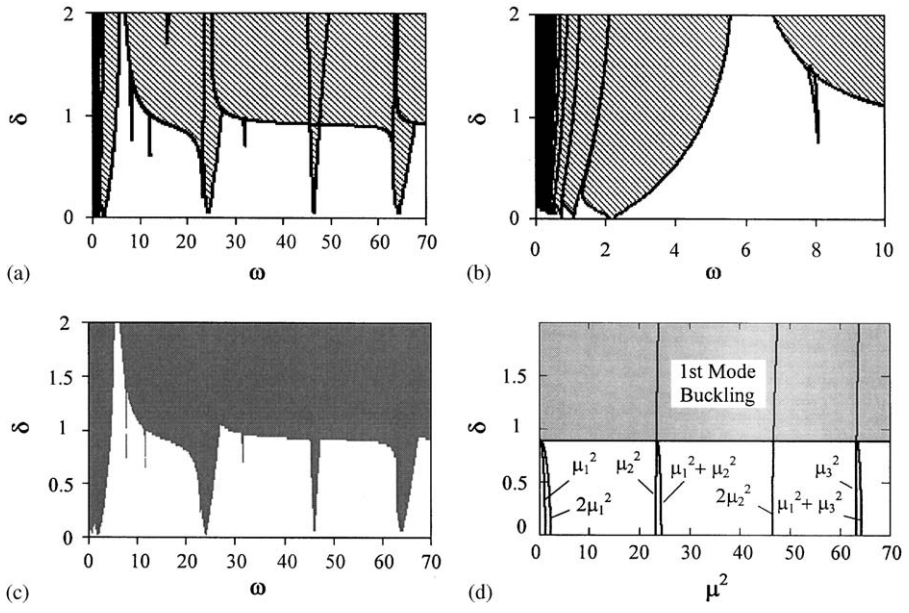

Fig. 8. Dynamic stability analysis: effect of speed fluctuation coefficient, inward-oriented beam; $\alpha = -0.4$, $\beta_0 = 5$ (a, b, generalized Bolotin method; c, monodromy matrix method; d, results from constant speed analysis).

6. Conclusions

Dynamic stability of rotating beams eccentrically clamped to a shaft with fluctuating speed is studied via both the generalized Bolotin and monodromy matrix methods.

The constant speed rotation problem is also reviewed and its reflections onto the fluctuating speed problem are underlined.

Along with its expected dynamic destabilizing effect, it is shown that a speed fluctuation may also have a stabilizing effect on statically unstable inward-oriented beams.

Although the driving shafts of the rotating blades (beams) are not allowed to undergo a substantial speed fluctuation in practice, such a situation may arise as a result of the torsional flexibility of the shaft. Therefore, it may be supposed that the outcomes of this study may also be useful in paving the way through the understanding of the coupled shaft torsional and blade bending vibrations of rotors.

Appendix A

The dimensionless natural frequencies of a stationary cantilever are the roots of the transcendental equation

$$1 + \cos\lambda \cosh\lambda = 0. \tag{A.1}$$

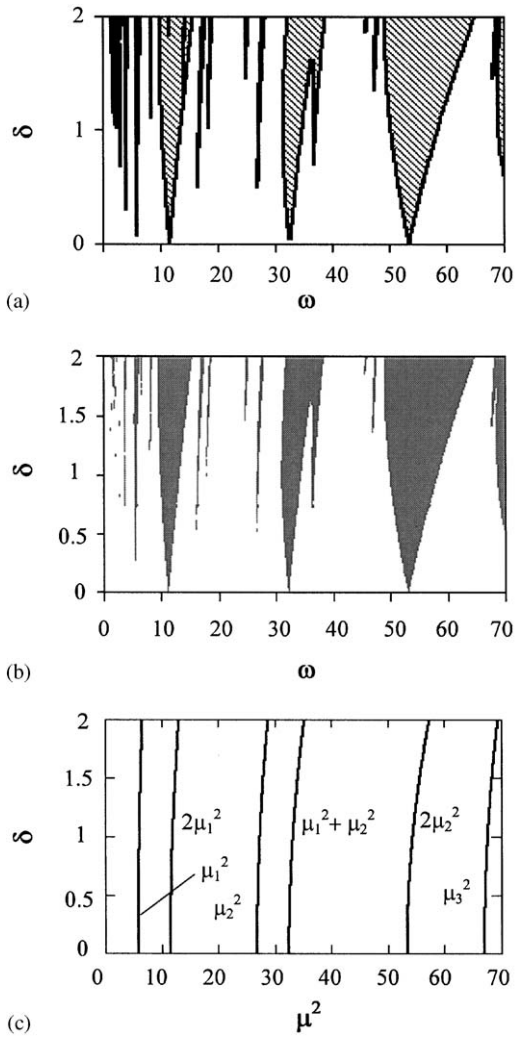

Fig. 9. Dynamic stability analysis: effect of speed fluctuation coefficient, outward-oriented beam; $\alpha = 0.4$, $\beta = 5$ (a, generalized Bolotin method; b, monodromy matrix method; c, results from constant speed analysis).

The first five of them are calculated as

$$\begin{aligned}\lambda_1 &= 1.87510407,\\ \lambda_2 &= 4.69409113,\\ \lambda_3 &= 7.85475744,\\ \lambda_4 &= 10.99554073,\\ \lambda_5 &= 14.13716839.\end{aligned} \tag{A.2}$$

Thus, according to Eq. (13) one has for $n=5$

$$\mathbf{A}=\begin{bmatrix} -1.57087819 & & & & \\ 0.42232039 & -8.64714269 & & \text{symmetric} & \\ 1.07208483 & -1.89005471 & -24.95211331 & & \\ 0.87313772 & 3.64338461 & -8.33828978 & -51.45910508 & \\ 0.76232572 & 3.06280535 & 7.14108671 & -19.01912840 & -87.79232739 \end{bmatrix}, \quad \text{(A.3)}$$

$$\mathbf{B}=\begin{bmatrix} -1.19333637 & & & & \\ 0.68585528 & -6.47822486 & & \text{symmetric} & \\ 0.79237922 & -0.16940788 & -17.85951988 & & \\ 0.54641327 & 2.91185111 & -3.27427206 & -36.05538833 & \\ 0.45407544 & 1.88916672 & 6.15441659 & -8.57015737 & -60.80107624 \end{bmatrix}, \quad \text{(A.4)}$$

$$\mathbf{c}=\{0.78299176 \quad 0.4339359 \quad 0.2544253 \quad 0.18189802 \quad 0.14147084\}^{\mathrm{T}}, \quad \text{(A.5)}$$

$$\mathbf{d}=\{0.56882574 \quad 0.09076679 \quad 0.03241637 \quad 0.01654234 \quad 0.01000703\}^{\mathrm{T}}. \quad \text{(A.6)}$$

References

[1] R.V. Southwell, Gaugh, The free transverse vibration of airscrew blades, British A.R.C. Report and Memoranda No. 766, 1921.

[2] M.J. Schilhansil, Bending frequency of a rotating cantilever beam, *Journal of Applied Mechanics* 25 (1958) 28–30.

[3] J.S. Rao, W. Carnegie, Non-linear vibrations of rotating cantilever beams, *The Aeronautical Journal of the Royal Aeronautical Society* 74 (1970) 161–165.

[4] W.D. Lakin, Vibrations of a rotating flexible rod clamped off the axis of rotation, *Journal of Engineering Mathematics* 10 (4) (1976) 313–321.

[5] S. Putter, H. Manor, Natural frequencies of radial rotating beams, *Journal of Sound and Vibration* 56 (2) (1978) 175–185.

[6] C.H.J. Fox, J.S. Burdess, The natural frequencies of a thin rotating cantilever with offset root, *Journal of Sound and Vibration* 65 (2) (1979) 151–158.

[7] A.D. Wright, C.E. Smith, R.W. Tresher, J.L.C. Wang, Vibration modes of centrifugally stiffened beams, *Journal of Applied Mechanics* 49 (1982) 197–202.

[8] R.B. Bhat, Transverse vibrations of a rotating beam with tip mass as predicted by using beam characteristic orthogonal polynomials in the Rayleigh–Ritz method, *Journal of Sound and Vibration* 105 (2) (1986) 199–210.

[9] M. Gürgöze, On the dynamical behaviour of a rotating beam, *Journal of Sound and Vibration* 143 (2) (1990) 356–363.

[10] S. Naguleswaran, Lateral vibration of a centrifugally tensioned uniform Euler–Bernouilli beam, *Journal of Sound and Vibration* 176 (5) (1994) 613–624.

[11] C.D. Eick, M.P. Mignolet, Vibration and buckling of flexible rotating beams, *AIAA Journal* 33 (3) (1995) 528–538.

[12] S. Naguleswaran, Out-of-plane vibration of a uniform Euler–Bernouilli beam attached to the inside of a rotating rim, *Journal of Sound and Vibration* 200 (1) (1997) 63–81.

[13] S.M. Hashemi, M.J. Richard, G. Dhatt, A new dynamic finite element (DFE) formulation for lateral free vibrations of Euler–Bernouilli spinning beams using trigonometric shape functions, *Journal of Sound and Vibration* 220 (4) (1999) 601–624.
[14] H.H. Yoo, S.H. Shin, Vibration analysis of rotating cantilever beams, *Journal of Sound and Vibration* 212 (5) (1998) 807–828.
[15] N. Mostaghel, I. Tadjbakhsh, Buckling of rotating rods and plates, *International Journal of Mechanical Sciences* 15 (1973) 429–434.
[16] F.G. Rammerstorfer, Comment on: Buckling of rotating rods and plates by N. Mostaghel and I. Tadjbakhsh, *International Journal of Mechanical Sciences* 16 (1974) 515–517.
[17] A. Nachman, The buckling of rotating rods, *Journal of Applied Mechanics* 42 (1975) 222–224.
[18] W.D. Lakin, A. Nachman, Unstable vibrations and buckling of rotating flexible rods, *Quarterly of Applied Mathematics* (1978) 479–493.
[19] W.F. White Jr., R.G. Kvaternik, K.R.V. Kaza, Buckling of rotating beams, *International Journal of Mechanical Sciences* 21 (1979) 739–745.
[20] D.A. Peters, D.H. Hodges, In-plane vibration and buckling of a rotating beam clamped off the axis of rotation, *Journal of Applied Mechanics* 47 (1980) 398–402.
[21] W.D. Lakin, R.G. Kvaternik, An integrating matrix formulation for buckling of rotating beams including the effects of concentrated masses, *International Journal of Mechanical Sciences* 31 (8) (1989) 569–577.
[22] Y.N. Al-Nassar, B.O. Al-Bedoor, On the vibration of a rotating blade on a torsionally flexible shaft, *Journal of Sound and Vibration* 259 (5) (2003) 1237–1242.
[23] Ö. Turhan, A generalized Bolotin's method for stability limit determination of parametrically excited systems, *Journal of Sound and Vibration* 216 (5) (1998) 851–863.
[24] B. Paul, *Kinematics and Dynamics of Planar Machinery*, Prentice-Hall, Englewood Cliffs, NJ, 1979.
[25] Ö. Turhan, Vibrations and stability of rotating beams with offset root, *Proceedings of the Tenth National Symposium on Theory of Machinery*, Konya, Turkey, Vol. 1, 2001, pp. 19–27 (in Turkish).
[26] L. Cesari, *Asymptotic Behavior and Stability Problems in Ordinary Differential Equations*, Springer, Berlin, 1959.
[27] A.T. Fuller, Conditions for a matrix to have only characteristic roots with negative real parts, *Journal of Mathematical Analysis and Applications* 23 (1968) 71–98.